Fermionic quantum dimer and fully-packed loop models on the square lattice

Frank Pollmann,[1] Joseph J. Betouras,[2] Kirill Shtengel,[3] and Peter Fulde[1,4]

[1]*Max-Planck-Institute for the Physics of Complex Systems, D-01187 Dresden, Germany*
[2]*Department of Physics, Loughborough University, Loughborough, Leicestershire LE11 3TU, UK*
[3]*Department of Physics and Astronomy, University of California, Riverside, California 92521, USA*
[4]*The Asia Pacific Center for Theoretical Physics, Pohang, Korea*

We consider fermionic fully packed loop and quantum dimer models which serve as effective low-energy models for strongly correlated fermions on a checkerboard lattice at half- and quarter-filling, respectively. We identify a large number of fluctuationless states specific to each case and which are due to fermionic statistics. We discuss the symmetries and conserved quantities of the system and show that, for a class of fluctuating states in the half-filling case, the fermionic sign problem can be gauged away. This claim is supported by a numerical evaluation of the low-lying states and can be understood by means of an algebraic construction. The elimination of the sign problem then allows us to analyze excitations at the Rokhsar-Kivelson point of the models using the relation to the height model and its excitations, within the single-mode approximation. We then discuss a mapping to a U(1) lattice gauge theory which relates the considered low-energy model to the compact quantum electrodynamics in $2 + 1$ dimensions. Furthermore, we point out consequences and open questions in the light of these results.

I. INTRODUCTION

Strongly correlated electrons on lattices with geometric frustration can lead to new physical properties. These come essentially from the quantum fluctuations acting on an extensively degenerate collection of classical ground states. From that point of view, strongly interacting spinless fermions (or, alternatively, fully spin-polarized electrons) on a frustrated lattice present an interesting example of this kind of physics. A spectacular consequence, for example, is that, at certain fillings, fractionally charged excitations have been predicted for the case of large nearest-neighbor repulsion on certain frustrated lattices.[1] The subject is not purely academic since there is experimental evidence that electrons in systems that have the considered lattice structure can be strongly correlated.[2,3] Furthermore, certain optical lattices with frustrated interactions can be produced by interfering laser beams and loaded with fermionic atoms. By varying the lattice constant, the strength of the correlations of the particles can be modified.[4]

In the present work we focus on the problem of strongly correlated electrons on a checkerboard lattice at two different filling fractions. This lattice can be seen as a two-dimensional (2D) projection of the pyrochlore lattice (three-dimensional tetrahedra are represented by 2D squares whose diagonals and sides are on an equal footing as far as couplings are concerned). We will consider the case of strong nearest-neighbor repulsion that favors the least possible number of fermions in each such square. At half-filling, this number is two, and an effective low-energy model maps onto a quantum fully packed loop (FPL) model on a square lattice. Some parts of this work have been briefly discussed before.[5,6] In the case of quarter-filling, a lowest potential energy arrangement corresponds to one fermion per square which can be mapped onto a hardcore dimer model. Here we supplement the study with further results and different aspects of the problem regarding the

symmetries and conserved quantities, the sign problem, and the corresponding gauge theories. We will discuss a number of consequences, especially related to the fermionic nature of the loops and dimers in this particular problem. Quantum dimer models (QDMs) have have been studied quite extensively in the past two decades.[7] Originally introduced in the context of quantum magnetism,[8] they became a focus of renewed interest following the discovery of a gapped quantum liquid phase on a triangular lattice.[9] It has been further established that a gapped topological phase with deconfined excitations generically exists in 2D for QDMs on nonbipartite lattices.[9–12] Such a phase has been found to have an effective description in terms of a Z_2 gauge theory.[13,14] By contrast, on bipartite lattices (e.g., a square lattice) there is a single deconfined quantum critical point separating phases of broken translation or rotation symmetry.[8,15–17] Such a point is characterized by a gapless excitation spectrum, which in turn leads to logarithmic confinement at any finite temperature. In both cases, QDMs can be mapped onto loop models with one significant difference: on a bipartite lattice the resulting loops can be naturally oriented whereas there is no natural notion of direction on a nonbipartite lattice. As a consequence, an effective gauge theory for a bipartite case is now a U(1) theory (the oriented loops can be though of as field lines in the absence of sources).[13,14] In addition, oriented loops naturally lend themselves to a height representation whereby they serve as contour lines. Several related models, such as the quantum six- or eight-vertex models in 2D have been shown to conform to the same dichotomy: a model with orientable loops is either ordered or critical and is described by a U(1) gauge theory while nonorientable quantum loops can result in a deconfined topological phase.[18–21] In all these models, the Hilbert space typically separates into disconnected subspaces corresponding to various conserved quantum numbers. When these quantum numbers are of nonlocal topological nature, such as winding numbers, the corresponding subspaces are referred to as topological sectors. While a Z_2 topological

phase is characterized by four such sectors and a corresponding four-fold ground-state degeneracy on a torus, the U(1) models have a much larger number of conserved quantities.

All aforementioned models share one important feature: all off-diagonal matrix elements connecting various quantum dimer or quantum loop states are nonpositive (or can be made nonpositive by a trivial gauge transformation such as associating a phase to dimers at certain locations). Within each disconnected sector the Hamiltonian dynamics is ergodic in the following sense: every two quantum states form a nonzero matrix element with some power of the Hamiltonian. (Here we are not concerned with the issue of how such a power may depend on the system size—a question that is essential for understanding the spectral gap or lack thereof.) The Perron-Frobenius theorem can then be applied to $\exp(-\tau H)$ for some positive τ within each disconnected subspace; it follows that the ground state for each sector is unique and nodeless.[9,22]

Much less is known about models with non-Frobenius dynamics, which result in some positive matrix elements. A striking difference between Frobenius vs. non-Frobenius QDMs on the kagome lattice was found in Refs. [12] and [27]: while the conventional QDM exhibits a gapped Z_2 topological phase, its counterpart with different signs has an extensive ground-state (GS) degeneracy. A different class of non-Frobenius lattice models has also been studied recently: fermionic models with supersymmetric Hamiltonians. In a number of cases such systems have been shown to have an extensive GS degeneracy.[23–26] From these examples, it appears that the non-Frobenius dynamics are often the source of additional quantum frustration resulting in the extensive ground-state entropy.

The goal of the present manuscript is to present a number of results (and some open questions) related to another non-Frobenius model that was originally introduced in Refs. [6] and [28]. The paper is organized as follows: We begin by introducing the considered model and derive an effective low-energy Hamiltonian in the following section. In Sec. III, we begin by analyzing the conservation laws specific to both quarter- and half-filled cases and the constraints they impose on the quantum dynamics. We discuss the nature of the sign problem and present two different approaches to alleviating it. In Sec. IV we extend the model by adding an extra term in the effective Hamiltonian that punishes flippable configurations. In such an extended model, we analyze in detail the Rokshar-Kivelson (RK) point and discuss the phase diagram. In Sec. V, we discuss the gauge theory for both the quarter-filled and the half-filled cases. We conclude and summarize our results in Sec. VI.

II. THE MODEL

Our starting Hamiltonian for spinless fermions is of the following form:

$$H = -t \sum_{\langle i\ j\rangle} (c_i^\dagger c_j + \text{H.c.}) + V \sum_{\langle i\ j\rangle} n_i n_j, \qquad (1)$$

where the summation is performed over neighboring sites of a checkerboard lattice. We are interested in the strongly interacting limit $V \gg t > 0$. Note that each site has six nearest

neighbors as in the pyrochlore lattice. The configurations favored by the interaction term depend on the doping (i.e., on the ratio of the number of particles to the number of the available sites). The fact that the particles are spinless fermions automatically prohibits double occupancy of sites. Furthermore, the interaction term favors uniform minimization of the number of such fermions on every crisscrossed square; a "planar tetrahedron." We will be mostly interested in a case of half-filling whereby the potential energy term is minimized whenever there are two fermions on each "planar tetrahedron," as shown in Figs. 1(a) and 1(b) (the tetrahedron rule[29]). The other case considered in parallel with the half-filling case in this work is that of quarter-filling, whereby the interaction energy is minimized by having one fermion per tetrahedron, as shown in Figs. 1(c) and 1(d).[5] In either case, configurations satisfying these rules can be represented by FPLs or dimers on a square lattice connecting the centers of the planar tetrahedra. The particles are sitting in the middle of the bonds of the square lattice. At half-filling, the tetrahedron rule translates into an FPL covering. By the same token, at quarter-filling, the minimum-interaction-energy manifold is spanned by the dimer coverings of the square lattice such that each site belongs to one and only one dimer. In either case, all other configurations are separated by a potential energy gap of at least V. Different FPL or dimer configurations are orthogonal to each other since they correspond to different locations of fermions (here we assume that these locations simply label the orthonormal set of Wannier functions).

(a) Two-particle exchange at half-filling

(b) Three-particle exchange at half-filling

(c) Two-particle exchange at quarter-filling

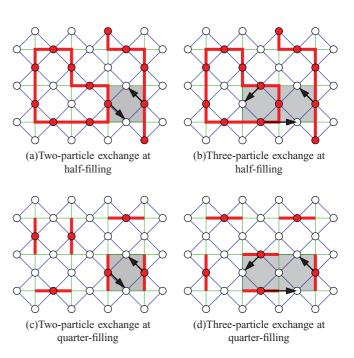(d) Three-particle exchange at quarter-filling

FIG. 1. (Color online) Panels (a) and (b) show a configuration of fermions satisfying the "two-per-tetrahedron" rule at half-filling and its representation in terms of FPLs. Panels (c) and (d) show configurations of fermions satisfying the "one-per-tetrahedron" rule at quarter-filling and their representations in terms of quantum dimers. In both cases, "flippable plaquettes" corresponding to two- and three-particle ring exchanges are shaded (see text for details).

At both half- and quarter-filling, the kinetic term in the Hamiltonian (1) moves particles between the neighboring sites, thus creating configurations in which the respective tetrahedron rules are violated. However, we are interested in the physics at the energy scale much smaller than V and therefore should look at the correlated multiparticle hops (ring exchanges) instead. The lowest-order process that does not take the system out of the low-energy manifold is the two-particle ring exchange depicted in Figs. 1(a) and 1(c). Such a process represents the dominant quantum dynamics for bosonic systems as well as for resonating valence bonds in spin systems.[8] However, its amplitude vanishes identically for fermions: the relative signs of clockwise and counterclockwise processes are opposite as a consequence of the fermionic exchange statistics, so the two contributions cancel each other. Moreover, the same observation holds for all ring exchanges involving any even numbers of fermions; the contributions from clockwise and counterclockwise moves of an even number of fermions that similarly cancel. Therefore, the shortest allowed fermionic ring exchanges involve three particles rather than two [see Figs. 1(b) and 1(d)]. Note that such cancellations of even ring exchanges is not a universal property but depends on the lattice. For example, distorting a square lattice (where the dimers live) into a rhombic lattice will change the relative amplitudes of clockwise and counterclockwise exchanges so that their contributions will no longer cancel. Furthermore, if the spin is included, processes of order t^2/V no longer vanish: two electrons with opposite spin can resonate around empty plaquettes of the checkerboard lattice and lower the energy.[30–32] By projecting the full Hamiltonian of Eq. (1) onto the Hilbert subspace restricted by the tetrahedron rules, we can perturbatively obtain an effective ring-exchange Hamiltonian that acts within such a subspace.[33] To lowest nonvanishing order in t/V, such an effective Hamiltonian becomes

$$H_{\text{eff}}^{(1/4)} = g \sum_{\{\square,\boxminus\}} \left(|\,\cdots\,\rangle\langle\,\vdots\,| + \text{H.c.} \right) \tag{2}$$

$$\equiv g \sum_p \left(|A\rangle\langle\overline{A}| + |\overline{A}\rangle\langle A| \right) \tag{3}$$

at quarter-filling and

$$H_{\text{eff}}^{(1/2)} = g \sum_{\{\square,\boxminus\}} \left(|\,\cdots\,\rangle\langle\,\vdots\,| + \text{H.c.} \right)$$
$$\quad - g \sum_{\{\square,\boxminus\}} \left(|\,\cdots\,\rangle\langle\,\vdots\,| + \text{H.c.} \right) \tag{4}$$

$$\equiv g \sum_p \left(|A\rangle\langle\overline{A}| + |\overline{A}\rangle\langle A| - |B\rangle\langle\overline{B}| - |\overline{B}\rangle\langle B| \right) \tag{5}$$

at half-filling. Here the sums are performed over all polygons of perimeter six and $g = 12t^3/V^2$. As we have already mentioned, the actual fermions are located at the centers of the dimers. The different relative signs of two terms at a half-filling sign result from the number of permuted fermions. It is either even or odd, which in turn depends on whether the middle site of the hexagon is occupied or empty. By contract, all ring exchanges come with the same sign in the case of the quarter-filling, as they all correspond to an empty middle site.

We should also point out that, while the sign of the coupling constant g is determined by the sign of t, it can be effectively changed by the following local gauge transformation: multiply a state by a factor of -1 for each vertical dimer in columns numbered $4k$ and $4k + 1$ (where $k \in \mathbb{Z}$) and do the same for horizontal dimers replacing columns by rows. A simple check shows that all ring-exchange terms in Eqs. (3) and (5) change their sign as a result. (It is worth noting that any diagonal; that is, potential energy terms, that one might consider adding to these Hamiltonians would remain intact under this gauge transformation.) Therefore, despite all appearances to the contrary, the quantum dynamics in Eq. (3) is not non-Frobebious. Such a gauge transformation, however, does not fix the relative sign of the different ring-exchange terms in Eq. (5)—this issue will be addressed in the following section.
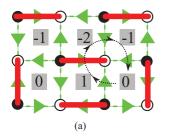
III. QUANTUM DYNAMICS

In this section, we discuss several aspects of the effective low-energy Hamiltonians which were derived in the previous section.

A. Conserved quantities

Our first observation is that, both at quarter- and half-filling, the low-energy Hilbert space of our model can be represented by height configurations. This follows from the aforementioned geometric representations of the ground states of the potential energy term in Eq. (1). For the case of quarter-filling they are the dimer coverings of the square lattice while for the case of half-filling they form FPLs on the same lattice, which are isomorphic to six-vertex configurations.[34] (The mapping between FPL and six-vertex configurations is done by subdividing the square lattice into even and odd sublattices and orienting occupied bonds from odd to even sites, with the opposite orientation for vacant bonds). Both dimer coverings and six-vertex configurations can in turn be mapped onto configurations of an interface—a so-called height representation, also known as a solid-on-solid (SOS) model.[35–37] Figures 2(a) and 2(b) show one of the ways of assigning heights to the plaquettes of the square lattice for both dimer coverings and FPL configurations.

The quantum dynamics that preserve these geometric constraints then result in quantum fluctuations of the local height variable. Hence our model is a variant of a quantum height model.[38,39] Let us begin by reiterating some results known from studies of bosonic quantum dimer models[38,39] and quantum six-vertex models.[18,19,21] A conservation law which is valid for the ring exchanges of any finite length is the conservation of the global slope of the height field. The global slope variable has two components, $\kappa_x(y)$ and $\kappa_y(x)$ in the x and y directions, respectively, which form a set of conserved numbers. (For the case of periodic boundary conditions, these can be immediately translated into the winding numbers.) There are two immediate consequences of this conservation law. The first one concerns the ergodicity of the quantum dynamics. Even for arbitrary local ring exchanges, the configurations corresponding to the different topological sectors (i.e., different overall slopes) cannot be mixed. Second, certain configurations; namely, those corresponding to a maximal possible slope in at least one direction, must be frozen since any local change in the height field would result in exceeding
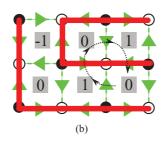
FIG. 2. (Color online) Recipe of how to map dimer and FPL coverings to a height model. First the links of the bipartite square lattice are oriented in such a way that the arrows are always pointing from the black to the white sublattice. Next we start from one arbitrary plaquette and set its value to zero. We then set the height value of the other plaquettes in the following ways: (a) Dimer model: If the traversed link is empty, we change the height by $\Delta h = 1$ if the arrow is from left to right and by $\Delta h = -1$ if the arrow is from right to left. If the traversed link is occupied by a dimer, we change the height by $\Delta h = -3$ if the arrow is from left to right and by $\Delta h = 3$ if the arrow is from right to left. The dashed line shows one possible path assigning the heights to the plaquettes. (b) FPL model: The rules are nearly identical to those for dimers except that $|\Delta h| = 1$ for both occupied and empty links. Since an FPL state is always an overlap of two dimer states, one can also obtain the same heights by simply adding those corresponding to the dimer states and dividing the result by two.

the maximal possible value of the step somewhere around the affected plaquette(s).

For the fermionic variants of the FPL and dimer models, there are two important differences which result from fermionic statistics. First, only ring exchanges involving odd numbers of particles are allowed (as discussed in Sec. II). In particular, the smallest resonating plaquette has perimeter six, rather than four, as captured by Eqs. (5) and (3), and thus the height updates involve two neighboring plaquettes rather than a single one. From the point of view of the fundamental conserved quantity of quantum height models—the global slope $\kappa_x(y)$ and $\kappa_y(x)$ of the height field—this difference is immaterial since the overall slope cannot be changed by any local dynamics. In addition, there is an accidental symmetry in our model, specific to the quantum dynamics in our case and that separately conserves the total numbers of vertical and horizontal dimers (moreover, it conserves the number of horizontal dimers in even and odd rows separately, and similarly for the vertical dimers). Hence, all states can be classified with respect to these quantum numbers which are different from the aforementioned conserved slopes. Notice that these additional conservation laws will not hold if higher-order ring-exchange terms are added to the effective Hamiltonian.

Second, the sign of the ring-hopping term in the fermionic FPL model depends on the occupancy of the middle bond. Both differences have important implications: the first one for the ergodicity of the quantum dynamics, while the second one leads to a sign problem in the quantum Monte Carlo dynamics. As we will see in the following subsection, the sign problem can be cured in certain cases. We note that the overall sign of H_{eff} (i.e., the sign of g) in Eqs. (5) and (3) is a matter of convention (as has been pointed out in Ref. 8 for the related

bosonic QDM). Introducing a factor of i for each vertical dimer in an odd row of the square lattice and for each horizontal dimer in an odd column changes this sign.

B. Sign problem: topological approach

We will now address the sign problem manifested by the opposite signs of the $A \leftrightarrow \overline{A}$ and $B \leftrightarrow \overline{B}$ terms in Eq. (5) and show that it can be avoided in certain (but not all) cases. Let us consider the surface with an even number of fermions remaining fixed at the boundary ("fixed" boundary conditions). Then fermion configurations are represented by closed loops as well as arcs terminating at the boundary. With no fermions at the boundary, there are closed loops only, as shown in Fig. 3(a). We add orientations to the loops as follows: (i) color the areas separated by the loops white and gray, with white being the outmost color; (ii) orient all loops so that the white regions are always to the right. In the presence of arcs [Fig. 3(b)], we can choose how to close them on the outside without intersections (the outside region has no dynamics). Letting white be the color at infinity, we orient the loops as described above.

We now consider how the effective Hamiltonian affects the loops covering. We first notice that the $B \leftrightarrow \overline{B}$ processes do not change the loop topology (or their number) while $A \leftrightarrow \overline{A}$ flips always do, with the possibilities presented schematically in Figs. 3(c) and 3(d). The relative signs resulting from the $A \leftrightarrow \overline{A}$ flips are consistent with multiplying each loop configuration by $i^l(-i)^r$, where r (l) is the number of the (counterclockwise) clockwise winding loops. Hence, by simultaneously changing the sign of the $A \leftrightarrow \overline{A}$ flips and transforming the loop states $|\mathcal{L}\rangle \to i^{l(\mathcal{L})}(-i)^{r(\mathcal{L})}|\mathcal{L}\rangle$, we cure the sign problem, thus making the system effectively bosonic.

Note that this construction need not work for the periodic boundary conditions. First, only even-winding sectors on a torus allow two-coloring. Secondly, even for even windings, we can start from a given configuration and find sequences of hexagon-flipping processes which invert the coloring when returning to the initial configuration (not shown here). This means that it is possible to dynamically reverse the coloring while and thus the sign gauging fails for these cases. It appears, however, that for the periodic boundary conditions on even tori (preserving the bipartiteness of the lattice), the lowest-energy states belong to the sector where such a transformation works, as confirmed by the exact diagonalization results [Fig. 4(a)].

The presented nonlocal loop-orienting construction is furthermore restricted to the ring-exchange processes of length six. The next-higher nonvanishing terms result from processes involving five fermions hopping around a polygon of length 10. The fact that the above-derived rules for the sign change due to the processes involving three fermions are violated can be seen from a counter example shown in Fig. 4(b). Here the five fermions hop around an odd number of fermions in the middle and thus yield a sign change. However, the fifth-order process here does not change the number or the orientation of the loop. Consequently, the sign gauging based on the topology of the loops breaks down once these terms are included.
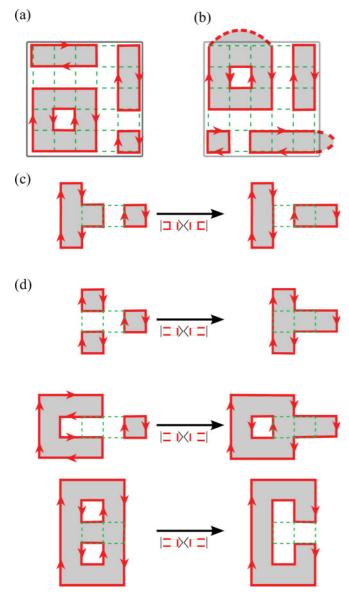
(a)

(b)

FIG. 4. (Color online) (a) GS energy and energies of lowest excited states of the effective Hamiltonian in sectors with different slopes $(\kappa_x, 0)$. Left panel: Data from an exact diagonalization of H_{eff} on a 72-site cluster where the Fermi sign is taken into account. Right panel: Same data from a calculation with excluded Fermi signs. (b) Counter example of a fifth-order process which changes the sign of the wave function but not the topology of the covering loops.

FIG. 3. (Color online) Panels (a) and (b) show the representation of the configuration as fully packed directed loops. (c) Action of a "non-sign-changing" process of the effective Hamiltonian. (d) Three different actions of "sign changing" processes on the topology of loop configurations.

C. Sign problem: algebraic approach

So far, we have attacked the sign problem using topological and computational arguments. In order to complement these approaches with an algebraic expression of the gauge transformation, we are seeking a possible way of representing the Hamiltonian (5) with the kinetic part in such a way that the "sign problem," which is manifested in the relative sign of the two terms, disappears.

We use gray-and-white coloring of the plane as has been discussed above. The two distinct possibilities of coloring a flippable rectangle (up to an overall color reversal) are shown in Fig. 5. Notice that, in both cases, both plaquettes forming a flippable rectangle (marked by the crosses) change their colors as a result of a "flip." The key observation, however, is that in
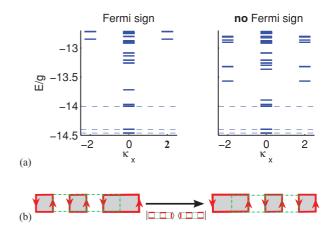
one case the color of these plaquettes is different and in the other it is the same.

Let us define an SU(2) "isospin" σ defined on each plaquette so that the eigenvalue $\sigma^z = \pm 1$ indicates whether the plaquette is white or gray, respectively. We can then rewrite the Hamiltonian (5) in terms of these new variables:

$$H_{\text{kin}} = g \sum_{\langle i,j \rangle} \sigma_i^z \sigma_j^z \sigma_i^x \sigma_j^x \Delta_{\text{flip}}(\sigma^z). \qquad (6)$$

We will now discuss the terms and show that (6) is a good representation of the original effective Hamiltonian. The operators $\Delta_{\text{flip}}(\sigma^z)$ is a projector which annihilates a state unless a legal flippable configuration exists in the plaquette pair (i,j), in which case its eigenvalue is 1. The explicit form of $\Delta_{\text{flip}}(\sigma^z)$ is complicated, but what is important is that it can
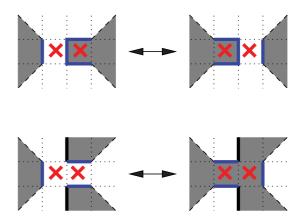

FIG. 5. (Color online) Two distinct "plaquette flips" and corresponding colorings of the plane. The two moves are different by the relative "−" sign. The dashed diagonal lines represent either of the two equivalent (for the purpose of our argument) locations of a dimer along one of the adjacent sides of a square. The red crosses indicate the double plaquette around which the loop segments resonate.

only depend on the σ^z of the two affected plaquettes and their neighbors. (This is just a formal consequence of the fact that, if we can look at the coloring and tell a flippable configuration from a nonflippable, there should be an operator that can do the same thing by "measuring" such coloring which in turn is uniquely determined by the values of σ^z). If $\Delta_{\text{flip}}(\sigma^z)$ returns 1 upon acting on a configuration, then the operators $\sigma_i^x \sigma_j^x$ simply flips the two isospins (i.e., flips the colors of both plaquettes), which means that it inverts the colors of the two plaquettes. The operator $\sigma_i^z \sigma_j^z$ determines the overall sign of this flip by distinguishing the two cases shown in Fig. 5. In other words, it yields the sign change which occurs in the B processes and represents the sign problem that we are attempting to tackle!

The resolution of the sign problem in the chosen representation is actually trivial: $\sigma^z \sigma^x = i\sigma^y$. Therefore,

$$H_{\text{kin}} = -g \sum_{\langle i,j \rangle} \sigma_i^y \sigma_j^y \Delta_{\text{flip}}(\sigma^z). \tag{7}$$

But the only "physical" direction in the isospin space is z, which corresponds to the plaquette being gray or white. The choice of x and y directions is a "gauge" choice. Hence we can always do a rotation around the z axis, so that $y \to x$ [in fact, we should rotate $y \to \pm x$ for the sites of the even or odd sublattice in order to consume the extra minus sign in Eq. (7)]. The result is

$$H_{\text{kin}} = g \sum_{\langle i,j \rangle} \sigma_i^x \sigma_j^x \Delta_{\text{flip}}(\sigma^z). \tag{8}$$

which is precisely Eq. (6) but without the different signs! Notice that this "spin rotation" affects the phases of the wave functions (written in σ^z representation). This construction coincides with the "loop transformation" we have presented earlier.

The nonlocal nature of this transformation is obvious from the fact that the σ are nonlocal operators:

$$\sigma_i^z = \exp\left[i\pi \sum_{k \in \mathcal{C}} c_k^\dagger c_k\right], \tag{9}$$

where $\mathcal{C}$ is a cut going from the given plaquette to the boundary (assumed white for simplicity), and $c_k^\dagger$ and c_k are creation and annihilation operators, respectively, for fermions at wave number k. The sum $\sum_{k \in \mathcal{C}} c_k^\dagger c_k$ simply counts the number of dimers crossing this cut (i.e., the number of fermions on the cut). This is actually identical to the Jordan-Wigner transformation in one dimension (1D)! This suggests that our model is "secretly" 1D-like, which explains why the fermionic sign can be gauged away. Notice that this nice property appears to be a consequence of restrictive three-particle dynamics described by Eq. (5); adding five-particle ring-exchanges seems to lead to a genuine sign problem that cannot be similarly fixed by a gauge transformation.

IV. ROKHSAR-KIVELSON POINT

Numerous examples demonstrate that a Hamiltonian containing only kinetic plaquette-flip (or ring-exchange) terms leads to an ordered phase stabilized by the "order-by-disorder" mechanism. On a square lattice, both the usual QDM and

the quantum six-vertex (FPL) models are at their plaquette phase[20,21,40,41] characterized by a checkerboard pattern (half as dense for the QDM case) of resonating plaquettes which break translational but not rotational symmetry of the lattice. A very similar plaquette phase occurs on a honeycomb lattice,[42] where the dimer model and FPL models are simply dual to one another. Moreover, a somewhat more complicated broken-symmetry state of the quantum dimers, dubbed $\sqrt{12} \times \sqrt{12}$, has been found on a nonbipartite triangular lattice.[14,43] In the fermionic case at quarter- and half-filling, the Hamiltonian (5) has also been shown to have an ordered ground state and fractionally charged "weakly" confined excitations.[44,45]

In order to explore the possible quantum phases with fermionic ring exchanges, we follow the example of Ref. 8 and extend our model's parameter space by adding a potential term as follows:

$$H_{\text{eff}}'^{(1/4)} = \sum_p \left[-g(|A\rangle\langle\overline{A}| + |\overline{A}\rangle\langle A|) + \mu(|A\rangle\langle A| + |\overline{A}\rangle\langle\overline{A}|) \right] \tag{10}$$

for the quarter-filled case and

$$H_{\text{eff}}'^{(1/2)} = \sum_p \left[-g(|A\rangle\langle\overline{A}| + |\overline{A}\rangle\langle A| + |B\rangle\langle\overline{B}| + |\overline{B}\rangle\langle B|) \right.$$
$$\left. + \mu(|A\rangle\langle A| + |\overline{A}\rangle\langle\overline{A}| + |B\rangle\langle B| + |\overline{B}\rangle\langle\overline{B}|) \right] \tag{11}$$

for the half-filled case. Here we use the short-hand notations introduced in Eqs. (3) and (5) and in both cases applied the gauge transformations discussed in Sec. III B to change the sign of the coupling constant in front of the $A \leftrightarrow \overline{A}$ terms. The Rokhsar-Kivelson (RK) point corresponds to $\mu = g$ where the Hamiltonian can be written as a sum of projectors:

$$H_{\text{eff}}'|_{g=\mu} = g \sum_p \left[(|A\rangle - |\overline{A}\rangle)(\langle A| - \langle\overline{A}|) \right.$$
$$\left. + (|B\rangle - |\overline{B}\rangle)(\langle B| - \langle\overline{B}|) \right] \tag{12}$$

for the half-filled case. Only the the first line (i.e.,the A terms) are present for quarter-filling. The important feature of this Hamiltonian is that it is positive semidefinite, hence (i) a zero-energy state is automatically a ground state and (ii) such a state must be annihilated simultaneously by all projectors. The consequence of the fact that the gauge-transformed Hamiltonian is of the Frobenius type is that, for each subspace of states connected by the quantum dynamics, the equal-amplitude superposition of such states is a unique "liquid" ground state. There is, however, a separate class of additional ground states—those not connected to any other states. These states by definition have no flippable configurations and hence are trivially annihilated by Hamiltonian (12). We note that such "frozen" states remain zero-energy states of Hamiltonians (10) and (11) for all values of μ, and remain the ground states for all $\mu > g$ because these Hamiltonians retain their positive semidefinite nature in this region.

While the fermionic nature of our original Hamiltonian has been seemingly gauged away, leaving us with a Frobenius type, we should recall that it is still manifest in the fact that only odd ring exchanges are allowed. This has a profound consequence for frozen states. All bosonic frozen states (i.e., frozen under a single plaquette flip dynamics) remain frozen

in our case. This is immediately obvious on a superficial level: all rectangles flippable by either the $A \leftrightarrow \bar{A}$ or $B \leftrightarrow \bar{B}$ terms contain a flippable plaquette, so a state with no flippable plaquettes is impervious to the dynamics of Hamiltonians (10) or (11). On a deeper level, bosonic frozen states remain frozen under fermionic dynamics since they are unaffected by any local ring exchange [see Figs. 6(a) and 6(b)]. In the height language, these states maximize the slope in some direction, making any local dynamics impossible. There are typically $\sim 2^L$ such configurations, their exact number may depend on the boundary conditions. Such counting is easiest at half-filling where one may maximize the slope of an $L \times L$ system in either $\pm x$ or $\pm y$ direction, which still leaves one with a freedom of 2^L possible arrangements of steps in the other direction resulting in a 4×2^L number of frozen states. In the quarter-filled (QDM) case there are four staggered states of the type shown in Fig. 6(a) that maximize the slope in either the $\pm x$ or $\pm y$ direction, with the slope in the other direction automatically fixed to zero. Additional frozen states can be obtained by creating diagonal domain walls between horizontal and vertical staggered states. Once again, all these states remain frozen under any local dynamics, fermionic or bosonic.

The nontrivial consequence of the fermionic dynamics is the appearance of a large number of additional frozen states that is not related to maximizing the slope. In fact, many of these states are in the flat sector. Two such examples are presented in see Figs. 6(c) and 6(d). Both the columnar state of quantum dimers [Fig. 6(c)] and the analogous FPL state [Fig. 6(d)] actually maximize the number of flippable plaquettes, yet both are fluctuationless under any fermionic dynamics. These states (along with staggered states) are members of a larger family of frozen fermionic states shown in Figs. 6(e) and 6(f). At quarter-filling, any state with only horizontal or only vertical dimers clearly cannot be changed by the application of the $|A\rangle\langle\bar{A}|$ terms since such terms necessarily involve both horizontal and vertical dimers. Moreover, it is easy to show that any ring exchange consisting of alternating occupied and empty bonds will involve an even number of fermions in this state and thus is not allowed. There are 2×2^L such states. A similar logic dictates that all FPL states like that shown in Fig. 6(f) are frozen under any fermionic dynamics. Whenever the loops can be sorted into two sets (shown in red and blue) in such a way that an empty bond always connects loops belonging to different sets, all ring exchanges are necessarily even. The number of such states has been counted by us in Ref. 6 and shown to scale as 4^{L+1} for large L. A number of additional fluctuationless states with the same "bipartite" property of loops [see e.g., Figs. 6(g) and 6(h)] can be constructed, yet we were unable to systematically count them. Hence it remains an open question whether our RK point is characterized by a truly extensive GS entropy like that found in Ref. 27 or Refs. 23–26.

In particular, one wonders whether our model can be actually related to this latter class of supersymmetric models[23–26] in any simple way. In short, the supersymmetric Hamiltonians are constructed as

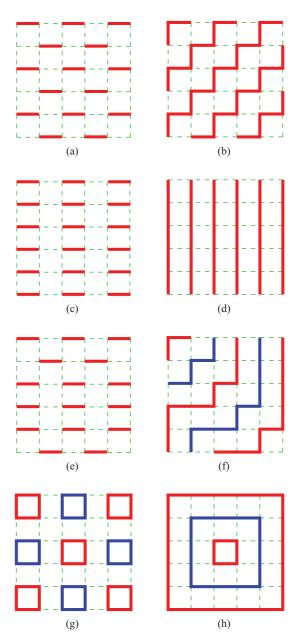$$H_{\text{SUSY}} = (Q + Q^\dagger)^2 = \{Q, Q^\dagger\}, \qquad (13)$$

FIG. 6. (Color online) Fragments of possible "frozen" states: (a,b) are fluctuationless under *any* local ring exchanges at quarter-filling (a) and half-filling (b); (c,d) are maximally flippable for bosonic, but fluctuationless for fermionic ring exchanges; (e,f) are the examples of generic fluctuationless configurations of fermions at both quarter-filling (e) and half-filling (f); (g,h) are other examples of fluctuationless configurations of fermions at half-filling.

where $Q^2 = Q^{\dagger 2} = 0$. It has been shown[23–26] that if one chooses $Q = \sum_i c_i P_{\langle i \rangle}$, where $P_{\langle i \rangle}$ projects out the states with fermions occupying sites adjacent to i, then such Hamiltonians may have an exponentially large number of zero-energy states (which are necessarily ground states). This conclusion, however, is sensitive to both the filling fractions and the underlying lattices. While the checkerboard lattice has actually been studied in this context[24] (under the name of "square dimer lattice") our Hamiltonian is clearly different. The ring-exchange terms can in fact be produced within this

framework by choosing $Q = \sum_{\langle\langle i,j,k,l,m,n\rangle\rangle}(c_i c_k c_m P_j P_l P_n \pm c_j c_l c_n P_i P_k P_m)$ where $P_i = 1 - n_i$; the sum is performed over all "flippable" rings consisting of sites i,j,k,l,m,n. The resulting supersymmetric Hamiltonian is both local and contains ring exchanges, yet it also contains other terms (including additional one- and two-particle hopping terms). What the relation is between the states of such a Hamiltonian and our Hamiltonian at its RK point is an interesting open question. A related question is whether our Hamiltonian can actually be written in a supersymmetric form by a more judicious choice of Q.

Whether or not this is the case, it remains quite suggestive that the explanation for the large number of additional frozen ground states lies in a more restrictive nature of the fermionic dynamics. We reiterate that these "new" frozen states are not related to any tilt constraints in the height language. The fact the frozen states now include the maximally flat states [Figs. 6(c) and 6(d)] is particularly interesting since they are supposed to dominate the ordered phase of both the quarter- and half-filled bosonic model for $\mu < \mu_c$ by maximizing the number of the flippable plaquettes. At quarter-filling, this is a columnar phase quantum dimers; $\mu_c \approx 0.6g$ numerically.[41] At half-filling, this is a conventional antiferroelectric phase of the six-vertex model referred to as the Néel phase in Ref. 20 and as DDW phase in Refs. 19 and 21; its upper boundary has been found to be $\mu_c \approx -0.374g$.[20] The aforementioned discussion makes it doubtful that such phases exist in the fermionic model. At half-filling, the phase dominated by a maximally flat configuration shown in Fig. 6(d) appears to be replaced by the somewhat analogous "squiggle" phase shown in Fig. 7(b).[44] In the quarter-filled case, the columnar phase appears to be replaced by a 2D analog of the "R state"[46,47] shown in Fig. 7(a).

A. Excitations at the Rokhsar-Kivelson point

The quantum dynamics of the Hamiltonian $H_{\rm eff}$ and similarly $H'_{\rm eff}$ can be described in terms of a height model as described above.[38] The associated conserved quantities κ_x and κ_y, as well as their insensitivity to a constant shift of the height field, imply gapless hydrodynamic modes with $\omega(k) \sim k^2$ as $k \to 0$. The liquid state of the FPL model at the RK point
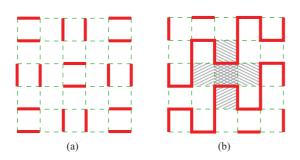

FIG. 7. (Color online) Fragments of states stabilized by quantum fluctuations. (a) The state maximizing the number of three-fermion ring exchanges at quarter-filling. (b) The "squiggle" state that maximizes the number of three-fermion ring exchanges at half-filling. The flippable rectangles involving the central plaquette are shaded.

corresponds to the rough phase of the height model, in which case the modes can be identified as the so-called resonons at wave vector (π,π)[8] and the equivalent of the pi0ns, here at $\mathbf{Q} = (0,0)$.[16,48,49] In the following we will elaborate on these physics.

For constructing gapless excitations in our model, we adopt the single-mode approximation (SMA),[50] which has been successfully used for the QDM on the square lattice.[8,16] A trial state with a momentum which differs from that of the ground state by $\mathbf{q}$ is constructed. The momentum is a good quantum number in a translationally invariant system. Then the variational principle employed on the states at that momentum yields the basic result that the energy of the trial state provides an upper bound on the excitation energy at that momentum. Therefore, as a matter of principle, one can use the SMA to prove gaplessness. In order to demonstrate the presence of a gap, a different method is needed.

Let $|0\rangle$ be one of the aforementioned "liquid" GSs at the RK point. The operator $d_{\hat{\tau}}^{+(-)}(\mathbf{r})$ creates (annihilates) a dimer at position $\mathbf{r}$ in direction (polarization) $\hat{\tau}$. The density operator $n_{\hat{\tau}}(\mathbf{r}) = d_{\hat{\tau}}^+(\mathbf{r})d_{\hat{\tau}}^-(\mathbf{r})$ has the Fourier transform $n_{\hat{\tau}}(\mathbf{q}) = \sum_{\mathbf{r}} n_{\hat{\tau}}(\mathbf{r})\exp(i\mathbf{q}\cdot\mathbf{r})$. We use the operators $n_{\hat{\tau}}(\mathbf{q})$ to construct the states $|\mathbf{q},\hat{\tau}\rangle = n_{\hat{\tau}}(\mathbf{q})|0\rangle$ which are, for $\mathbf{q} \neq 0$, orthogonal to $|0\rangle$. By using the variational method, the excitation energies $E(\mathbf{q},\hat{\tau})$ are bounded by

$$E(\mathbf{q},\hat{\tau}) \leqslant f(\mathbf{q})/S_{\tau\tau}(\mathbf{q}), \qquad (14)$$

where

$$f(\mathbf{q}) = \langle 0|[n_{\hat{\tau}}(-\mathbf{q}),[H'_{\rm eff},n_{\hat{\tau}}(\mathbf{q})]]|0\rangle \qquad (15)$$

is the oscillator strength and

$$S_{\hat{\tau}\hat{\tau}}(\mathbf{q}) = \langle 0|n_{\hat{\tau}}(-\mathbf{q})n_{\hat{\tau}}(\mathbf{q})|0\rangle \qquad (16)$$

is the structure factor, which is essentially the Fourier transformation of the dimer density correlation function.

It is important that both the oscillator strength and the structure factor can be evaluated as expectation values with respect to the ground state. The ground-state correlations encode information on the excitation spectrum and some of them can be captured by the variational method which leads to the above expression. The SMA is useful then because there are situations in which gaplessness is present in a generic manner. The behavior of $f(\mathbf{q})$ near $q \to 0$ can then be used to determine a bound on the dispersion of the soft excitations. A finite $f(\mathbf{q})$ accompanied by a divergence of the structure factor can be used to infer gapless excitations. Such a soft mode is a classic signature of incipient order.

In order to calculate $f(\mathbf{q})$, we observe that the density operators commute with the potential energy term, so only the kinetic energy term contributes. Let us first consider the case where $\hat{\tau} = \hat{x}$. By using the commutation relation $[d_{\hat{\tau}}^{\pm},n_{\hat{\tau}}] = \mp d_{\hat{\tau}}^{\pm}$ repeatedly, we compute $f(\mathbf{q})$ due to the resonating terms. The result for the necessary commutators in order to compute the oscillator strength are (for a square lattice with lattice spacing $a = 1$)

$$[n_{\hat{x}}(-(\mathbf{Q}+\mathbf{k})),[-gT_{\boxminus}^{A/B},n_{\hat{x}}((\mathbf{Q}+\mathbf{k}))]]$$
$$= 4gT_{\boxminus}^{A/B}e^{(i\mathbf{Q}\cdot\mathbf{R})}\sin^2[(\mathbf{Q}+\mathbf{k})\cdot\hat{y}] \qquad (17)$$

and

$$\left[n_{\hat{x}}\left(-(\mathbf{Q}+\mathbf{k}) \right), \left[-g T_{\boxminus}^{A/B}, n_{\hat{x}}\left((\mathbf{Q}+\mathbf{k}) \right) \right] \right]$$
$$= -4g T_{\boxminus}^{A/B} e^{(i\mathbf{Q}\cdot\mathbf{R})} \left[1 + \cos\left((\mathbf{Q}+\mathbf{k})\cdot\hat{y} \right) \right]$$
$$\times \left[(-1 + \cos\left((\mathbf{Q}+\mathbf{k})\cdot\hat{x} \right) \right], \qquad (18)$$

where $T_{\boxminus}^{A/B}$ and $T_{\boxminus}^{A/B}$ denote the resonant motion in the minimal ring-exchange process with double plaquettes oriented in a column or in a row and with the middle dimer occupied (A kind) or unoccupied (B kind).

If we write $\mathbf{k} = \mathbf{q} - \mathbf{Q}$ and consider $\mathbf{q}$ around three different values of $\mathbf{Q} = (0,0),(\pi,\pi),(0,\pi)$ (and therefore small k), then we can expand the results for the oscillator strengths. Then, to leading order we find that $f(\mathbf{k}) \sim (\mathbf{k} \times \hat{\tau})^2$, which is a similar type of expression as the one for the RK model.[8] Nevertheless, this result alone is not sufficient to give the whole information of the gapless excitations because the second necessary ingredient, the structure factor, can also be zero along the direction where $\mathbf{k}$ is zero.

Therefore, let us now consider the structure factor $S_{\hat{x}\hat{x}}(\mathbf{q})$ both for the FPL and dimer models independently. We use the expression given in Ref. 49. Interestingly, the main result is that $S_{\hat{x}\hat{x}}(\mathbf{q}) \neq 0$ except along the direction $\mathbf{q} = (q_x,\pi)$ where it vanishes with the exception of (π,π). At that point we have the gapless excitations termed "resonons" by RK. At $(0,\pi)$ both $f(\mathbf{q})$ and $S_{\hat{x}\hat{x}}(\mathbf{q})$ are zero, but their ratio remains finite. In addition, for the FPL $S_{\hat{x}\hat{x}}(\mathbf{q})$ shows no singularities. In that respect, the FPL model differs from the hardcore dimer model (describing our model at quarter-filling) for which $S_{\hat{x}\hat{x}}(\mathbf{q})$ diverges logarithmically at $\mathbf{Q} = (\pi,0)$.[16] The difference is due to a slower algebraic decrease with distance of the correlation function for hardcore dimer covering. The correlation function for the dimer model at distance r reads

$$C_{\hat{x}\hat{x}} \sim (-1)^{x+y}\frac{y^2 - x^2}{r^4} + (-1)^x\frac{1}{r^2}, \qquad (19)$$

whereas for the FPL model it decays with a characteristic exponent which is greater than 2.[51]

We have also verified the results for the structure factors of our model $S_{\hat{x}\hat{x}}(\mathbf{q})$ by means of Monte Carlo simulations for both cases, see Fig. 8(a) for the FPL model and Fig. 8(b) for the case of hard-core dimers. The results remain identical (and symmetrical in the indices involved) for the orientation $\hat{\tau} = \hat{y}$.

V. U(1) GAUGE THEORY

The effective Hamiltonian (5) conserves the number of particles on each crisscrossed square (i.e., the number of loops or dimers touching each site is conserved). This conservation generates a local U(1) gauge invariance, as it is usually the case in models with local constraints.[13] The gauge structure suggests that we can gain further insight with respect to low-energy excitations by writing our model as a U(1) lattice gauge theory. The usefulness of this approach has already been shown for the quantum dimer model (QDM) on the square lattice,[13] strongly correlated proton systems,[52] as well as for 3D spin systems.[53] The gauge theory can be derived for the dimer model as well as for the loop model in a very similar manner.
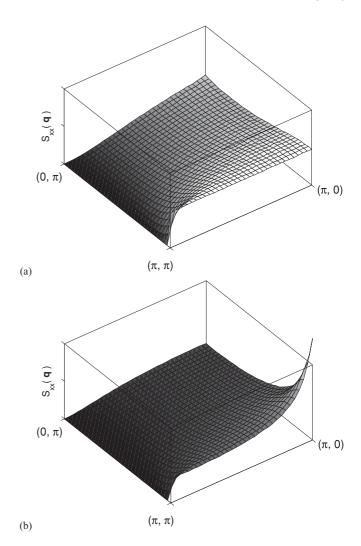

(a)

(b)

FIG. 8. Structure factor $S_{\hat{x}\hat{x}}$ for the (a) FPL and (b) hard-core dimers on the square lattice.

A. Dimer model

We start by defining an integer variable $n_j(\mathbf{x})$ for each link $(\mathbf{x}, \mathbf{x} + \hat{e}_j)$ of the square lattice. The coordinates of a lattice site are denoted by $\mathbf{x}$, and $\hat{e}_{j=1,2}$ are unit vectors along the axes as shown in Fig. 9. The states $|\{n_j(\mathbf{x})\}\rangle$ span an enlarged Hilbert space which has integer numbers for the links instead only zero or one. We can consider the states $|\{n_j(\mathbf{x})\}\rangle$ as eigenstates of quantum rotor operators $\hat{n}_j(\mathbf{x})$ with eigenvalues $n_j(\mathbf{x})$.
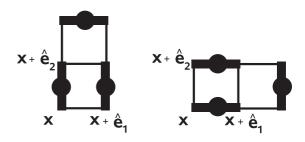

FIG. 9. Labeling of links on flippable double-plaquettes at position $\mathbf{x}$ with unit vectors $\hat{e}_1$ and $\hat{e}_2$.

In order to express the effective Hamiltonian in terms of the $\hat{n}_j(\mathbf{x})$, we introduce phases $\hat{\phi}_j(\mathbf{x}) \in [0,\pi)$ on the links which are canonical conjugate to $\hat{n}_j(\mathbf{x})$. Using the fact that $\exp[\pm i\hat{\phi}_j(\mathbf{x})]$ act as ladder operators, we can write

$$\mathcal{H}_{\text{eff}} = U \sum_{\mathbf{x},j} \left(\hat{n}_j(\mathbf{x}) - \frac{1}{2} \right)^2 - 2g \sum_{\{\boxempty,\boxplus\}} \cos \left[\sum \pm \hat{\phi} \right]. \quad (20)$$

Here, the argument of the cosine term contains the sum over phases $\hat{\phi}_j(\mathbf{x})$ with alternating signs around the polygons of perimeter six (double plaquettes). In the limit $U/g \to \infty$, all "nonphysical" states are projected out and Eq. (20) is a faithful representation of the effective Hamiltonian (3). Next, we introduce staggered gauge and electric fields on the bipartite square lattice $\mathbf{x} = (x_1, x_2)$ by

$$\hat{A}_j(\mathbf{x}) = (-1)^{x_1+x_2} \hat{\phi}_j(\mathbf{x}),$$
$$\hat{E}_j(\mathbf{x}) = (-1)^{x_1+x_2} \left(\hat{n}_j(\mathbf{x}) - \tfrac{1}{2} \right).$$

The local constraint that each site is touched by exactly one dimer reads

$$(\Delta_j \hat{E}_j(\mathbf{x}) - \rho(\mathbf{x}))|\text{Phys.}\rangle = 0, \quad (21)$$

with the staggered background charge

$$\rho(\mathbf{x}) = (-1)^{(x_1+x_2+1)}. \quad (22)$$

The lattice divergence is defined as

$$\Delta_j \hat{E}_j(\mathbf{x}) \equiv \hat{E}_1(\mathbf{x}) - \hat{E}_1(\mathbf{x} - \mathbf{e}_1) + \hat{E}_2(\mathbf{x}) - \hat{E}_2(\mathbf{x} - \mathbf{e}_2).$$

The dimer hardcore dimer constraint is now reflected by the standard Gauss' law (21) in the presence of a staggered background charge density. Using the staggered fields as defined above, the Hamiltonian (20) reads

$$\mathcal{H}_{\text{eff}} = U \sum_{\mathbf{x},j} \hat{E}_j^2(\mathbf{x}) - 2g \sum_{\mathbf{x}} \cos \left[\sum_{\mathsf{C}} \hat{A}_j(\mathbf{x}) \right]. \quad (23)$$

The argument of the cosine term denotes the oriented sum of staggered vector potentials $\hat{A}_j(\mathbf{x})$ around double plaquettes.

B. Loop model

Let us now consider the loop model which corresponds to the half-filled checkerboard lattice. The matrix-elements of the effective Hamiltonian (5) have different signs depending on whether the link in the middle is occupied or not. Using the gauge transformation presented in Sec. III B, we can rewrite the Hamiltonian in a representation which has only negative matrix elements and redo the derivation presented above for the dimer model. The only difference between the dimer and loop model is the form of Gauss' law, which reflects the loop constraint. Using the same notation as for the dimer model, the local constraint that each site is touched by exactly two dimers reads

$$\Delta_j \hat{E}_j |\text{Phys.}\rangle = 0. \quad (24)$$

Thus, the corresponding Gauss' law has no background charges.

Equation (23) has similarities with the Hamiltonian of the compact quantum electrodynamics (QED) in $2 + 1$ dimensions in which the considered charges correspond to fractional charges of $e/2$.[54] Polyakov showed for the compact QED in $2 + 1$ dimensions that it has a unique and gapped ground state. Two charges are confined and the energy grows linearly with the distance between the two charges. Our model shows important differences. The fields $E_j(\mathbf{x})$ are half-integers instead of integers and the constraint selects configurations with a background charge $\rho(\mathbf{x})$. This leads to a frustration, which is reflected by the macroscopic degeneracy of the classical ground states. Furthermore, the definition of the flux in the cosine term differs.

The formulation (23) provides an excellent starting point for further systematic investigations. The plaquette duality transformation allows us to map the Hamiltonian to a height model and to use path integrals for a detailed study of the ground state as well as low-energy excitations.[13]

VI. CONCLUSION

In this study, we analyzed in detail a model of strongly correlated spinless fermions on a checkerboard lattice both at half- and quarter-filling by mapping it onto a quantum dimer and quantum fully packed loop models on the square lattice, respectively. The lowest-order effective Hamiltonian is given by ring-hopping processes around hexagons which involve three fermions. The symmetries and conservations of the model were studied in detail. We found a large number of frozen states which are not related to any height constraints and are specific for the fermionic case. Using a topological and an algebraic approach, we showed that the sign problem induced by the fermion statistics in the half-filled case can be cured. We explained and studied different aspects of this observation and showed that it does not remain true when further ring-exchange processes are also taken into account. By adding an extra term to the Hamiltonian, we fine tuned the system to the Rokhsar-Kivelson point where the ground states are known exactly. Using the proposed sign gauging and the single-mode approximation, we argue that the Rokhsar-Kivelson point is a quantum critical point and that the system crystalizes once it is slightly detuned. Moreover, we mapped the system at both fillings to the corresponding gauge theories which dictates confinement of fractionalized defects created by an addition (or subtraction) of fermions.

Recent studies of other lattices such as kagome at $1/3$ fermionic filling concluded that the defects (in the form of fractional charges) are confined.[55] This is also the case in the present study and it is a consequence of the confined nature of the gauge theory, as explained above. The fact that the lattice under consideration is bipartite as well as the imposed local constraints lead to the fractionalization of the defects with protected values of the fractional charge (one half in we dope the system with an extra fermion).

Finally, we should caution the reader who may be left with an impression that, aside from the fact that only odd ring exchanges are present, the fermionic nature of the model considered here can be essentially "gauged away." Therefore,

it must be reiterated that the methods we have proposed are of somewhat limited applicability. First, they only work for special filling fractions. Their nongeneric nature is obvious from the fact that, for the quarter-filled case, a simple local gauge transformation would suffice to make the quantum dynamics of the Frobenius type, while for the half-filled case a far more complicated nonlocal transformation was required. Therefore, it would be extremely interesting to study this model away from these special fillings and to try to identify the features that are generic.

[1] P. Fulde, K. Penc, and N. Shannon, Ann. Phys. **11**, 892 (2002).

[2] S. Kondo *et al.*, Phys. Rev. Lett. **78**, 3729 (1997).

[3] F. Walz, J. Phys. Condens. Matter **14**, R285 (2002).

[4] D. Jocksch and P. Zoller, Ann. Phys. (NY) **315**, 52 (2005).

[5] F. Pollmann, J. J. Betouras, and E. Runge, Phys. Rev. B **73**, 174417 (2006).

[6] F. Pollmann, J. J. Betouras, K. Shtengel, and P. Fulde, Phys. Rev. Lett. **97**, 170407 (2006).

[7] R. Moessner and K. S. Raman (2008), e-print arXiv:0809.3051.

[8] D. S. Rokhsar and S. A. Kivelson, Phys. Rev. Lett. **61**, 2376 (1988).

[9] R. Moessner and S. L. Sondhi, Phys. Rev. Lett. **86**, 1881 (2001).

[10] C. Nayak and K. Shtengel, Phys. Rev. B **64**, 064422 (2001).

[11] P. Fendley, R. Moessner, and S. L. Sondhi, Phys. Rev. B **66**, 214513 (2002).

[12] G. Misguich, D. Serban, and V. Pasquier, Phys. Rev. Lett. **89**, 137202 (2002).

[13] E. Fradkin and S. A. Kivelson, Mod. Phys. Lett. B **4**, 225 (1990).

[14] R. Moessner, S. L. Sondhi, and E. Fradkin, Phys. Rev. B **65**, 024504 (2001).

[15] S. Sachdev, Phys. Rev. B **40**, 5204 (1989).

[16] R. Moessner and S. L. Sondhi, Phys. Rev. B **68**, 184512 (2003).

[17] E. Fradkin, D. A. Huse, R. Moessner, V. Oganesyan, and S. L. Sondhi, Phys. Rev. B **69**, 224415 (2004).

[18] E. Ardonne, P. Fendley, and E. Fradkin, Ann. Phys **310**, 493 (2004).

[19] S. Chakravarty, Phys. Rev. B **66**, 224505 (2002).

[20] N. Shannon, G. Misguich, and K. Penc, Phys. Rev. B **69**, 220403 (2004).

[21] O. F. Syljuåsen and S. Chakravarty, Phys. Rev. Lett. **96**, 147004 (2006).

[22] C. Castelnovo, C. Chamon, C. Mudry, and P. Pujol, Ann. Phys. **318**, 316 (2005).

[23] P. Fendley and K. Schoutens, Phys. Rev. Lett. **95**, 046403 (2005).

[24] H. van Eerten, J. Math. Phys. **46**, 123302 (2005).

[25] L. Huijse, J. Halverson, P. Fendley, and K. Schoutens, Phys. Rev. Lett. **101**, 146406 (2008).

[26] L. Huijse and K. Schoutens, Eur. Phys. J. B **64**, 543 (2008).

[27] G. Misguich, D. Serban, and V. Pasquier, Phys. Rev. B **67**, 214413 (2003).

[28] F. Pollmann, J. J. Betouras, E. Runge, and P. Fulde, J. Magn. Magn. Mater. **310**, 966 (2007).

[29] P. W. Anderson, Phys. Rev. **102**, 1008 (1956).

[30] D. Poilblanc, K. Penc, and N. Shannon, Phys. Rev. B **75**, 220503 (2007).

[31] D. Poilblanc, Phys. Rev. B **76**, 115104 (2007).

[32] F. Trousselet, D. Poilblanc, and R. Moessner, Phys. Rev. B **78**, 195101 (2008).

[33] E. Runge and P. Fulde, Phys. Rev. B **70**, 245113 (2004).

[34] E. H. Lieb and F. Y. Wu, *Phase Transitions and Critical Phenomena*, edited by C. Domb and M. S. Green (Academic Press, London, 1972), Vol. 1, pp. 331–490.

[35] H. van Beijeren, Phys. Rev. Lett. **38**, 993 (1977).

[36] H. W. J. Blöte and H. J. Hilborst, J. Phys. A: Math. Gen. **15**, L631 (1982).

[37] L. S. Levitov, Phys. Rev. Lett. **64**, 92 (1990).

[38] C. L. Henley, J. Stat. Phys. **89**, 483 (1997).

[39] C. L. Henley, J. Phys. Condens. Matter **16**, S891 (2004).

[40] P. W. Leung, K. C. Chiu, and K. J. Runge, Phys. Rev. B **54**, 12938 (1996).

[41] O. F. Syljuåsen, Phys. Rev. B **73**, 245105 (2006).

[42] R. Moessner, S. L. Sondhi, and P. Chandra, Phys. Rev. B **64**, 144416 (2001).

[43] A. Ralko, M. Ferrero, F. Becca, D. Ivanov, and F. Mila, Phys. Rev. B **71**, 224109 (2005).

[44] F. Pollmann and P. Fulde, Europhys. Lett. **75**, 133 (2006).

[45] F. Pollmann, Ph.D. thesis, Technische Universität Ilmenau [http://nbn-resolving.de/urn/resolver.pl?urn=nbn:de:gbv:ilm1-2006000140] (2006).

[46] D. L. Bergman, R. Shindou, G. A. Fiete, and L. Balents, Phys. Rev. Lett. **96**, 097207 (2006).

[47] O. Sikora, F. Pollmann, N. Shannon, K. Penc, and P. Fulde, Phys. Rev. Lett. **103**, 247001 (2009).

[48] R. Moessner and S. L. Sondhi, Phys. Rev. B **68**, 064411 (2003).

[49] R. Moessner, O. Tchernyshyov, and S. L. Sondhi, J. Stat. Phys. **116**, 755 (2004).

[50] R. P. Feynman, *Statistical Mechanics: A Set of Lectures* (Addison-Wesley, Reading, 1972).

[51] R. Raghavan, C. L. Henley, and S. L. Arouh, J. Stat. Phys. **86**, 517 (1997).

[52] A. H. Castro Neto, P. Pujol, and E. Fradkin, Phys. Rev. B **74**, 024302 (2006).

[53] M. Hermele, M. P. A. Fisher, and L. Balents, Phys. Rev. B **69**, 064404 (2004).

[54] A. M. Polyakov, Nucl. Phys. B **120**, 429 (1977).

[55] A. O'Brien, F. Pollmann, and P. Fulde, Phys. Rev. B **81**, 235115 (2010).